

REPORT DOCUMENTATION PAGE				Form Approved OMB No. 0704-0188	
<p>Public reporting burden for this collection of information is estimated to average 1 hour per response, including the time for reviewing instructions, searching existing data sources, gathering and maintaining the data needed, and completing and reviewing the collection of information. Send comments regarding this burden estimate or any other aspect of this collection of information, including suggestions for reducing the burden, to Department of Defense, Washington Headquarters Services, Directorate for Information Operations and Reports (0704-0188), 1215 Jefferson Davis Highway, Suite 1204, Arlington, VA 22202-4302. Respondents should be aware that notwithstanding any other provision of law, no person shall be subject to any penalty for failing to comply with a collection of information if it does not display a currently valid OMB control number.</p> <p>PLEASE DO NOT RETURN YOUR FORM TO THE ABOVE ADDRESS.</p>					
1. REPORT DATE (DD-MM-YYYY) 21-12-2000		2. REPORT TYPE Final Report		3. DATES COVERED (From - To) 26 April 2000 - 01-Jun-01	
4. TITLE AND SUBTITLE A mesoscale model for thin film production processes.			5a. CONTRACT NUMBER F61775-00-WE026		
			5b. GRANT NUMBER		
			5c. PROGRAM ELEMENT NUMBER		
6. AUTHOR(S) Professor Leslie V Woodcock			5d. PROJECT NUMBER		
			5d. TASK NUMBER		
			5e. WORK UNIT NUMBER		
7. PERFORMING ORGANIZATION NAME(S) AND ADDRESS(ES) Scientific Simulation Services 2 Brambling Drive BRADFORD BD6 3XB United Kingdom			8. PERFORMING ORGANIZATION REPORT NUMBER N/A		
9. SPONSORING/MONITORING AGENCY NAME(S) AND ADDRESS(ES) EOARD PSC 802 BOX 14 FPO AE 09499-0014			10. SPONSOR/MONITOR'S ACRONYM(S)		
			11. SPONSOR/MONITOR'S REPORT NUMBER(S) SPC 00-4026		
12. DISTRIBUTION/AVAILABILITY STATEMENT Approved for public release; distribution is unlimited.					
13. SUPPLEMENTARY NOTES					
14. ABSTRACT <p>This report results from a contract tasking Scientific Simulation Services as follows: Contractor will develop a computer model used to obtain otherwise inaccessible "experimental" information on the properties of thin colloidal films as a function of the rate of production process parameters. A thorough literature survey report will be prepared of all the experiment methods currently available for the synthesis of monodisperse particulates, organic polymers, synthetic bio colloids and inorganic ceramic oxides. Exploratory laboratory tests will also be made to synthesise 532nm polystyrene latex and pmma particles for comparison with model results. Additional information is contained in the proposal statement of work.</p>					
15. SUBJECT TERMS EOARD, Materials <div style="text-align: right; font-size: 2em; font-weight: bold; margin-top: 20px;">20020108 142</div>					
16. SECURITY CLASSIFICATION OF:			17. LIMITATION OF ABSTRACT UL	18. NUMBER OF PAGES 34	19a. NAME OF RESPONSIBLE PERSON Carl A. Kutsche
a. REPORT UNCLAS	b. ABSTRACT UNCLAS	c. THIS PAGE UNCLAS			19b. TELEPHONE NUMBER (include area code) +44 (0)20 7514 4505

FINAL REPORT

United States Air Force Research Contract SPC 00-4026

A mesoscale model for thin film production processes

Summary: A mesoscale computer program in FORTRAN 90, titled MNCELL.f, and derivative programs, MNSLAB.f, and IONCELL.f have been developed [1] and tested for simple particulate models with inverse-power (m-n) attractive with repulsive core potentials. The programs simulate the continuous steady-state production of solids and thin colloidal films using periodic boundaries. The programs incorporate a new, more efficient, method of particle neighborhood indexing. Experimental non-intrusive methods of monitoring colloidal rheology are reviewed. A literature survey submitted earlier for the production of monodisperse colloids is revised. A laboratory test facility has been put in place to produce to specification monodisperse latex particles with a prescribed sub-micron mean particle diameter.

Declaration of Technical data Conformity

The Contractor Scientific Simulation Services hereby declares that, to the best of its knowledge and belief, the technical data delivered herewith under Contract number F61775-00-WE026 is complete, accurate and complies with all requirements of the contract.

Date: 19 December 2000

Professor Leslie V Woodcock
Scientific Simulation Services.

I certify that there were no subject inventions to declare as defined in FAR 52-2227-13 during the performance of this contract.

Date 19 December 2000

Professor Leslie V Woodcock
Scientific Simulation Services.

CONTENT

- 1) **Objectives**
- 2) **Uniaxial compaction in steady states**
- 3) **Simulations** a. MNCCELL.f
 b. MNLAB.f
 c. IONCELL.f
- 4) **Colloidal rheometry**
- 5) **Monodisperse colloid syntheses**

REFERENCES

APPENDIX I **MNLAB.f annotated**

APPENDIX II **Reagents list for monodisperse submicron latex particles.**

1) Objectives

The primary objective of the computational project is to develop a computer model to simulate the continuous production of a particulate solid film from a low density feed phase, by uniaxial compaction.

In the common process for the continuous production of a binary composite material, a powder is fed from a hopper, a second powder is fed from another hopper, both may mixed and with a liquid feed, or dry with gravity or a gas cyclone. The mixed colloidal suspension is then piped for processing to a solid material. Typically, at some later stage, the particles in the binary suspension are to be compacted to a dense solid state. The uniaxial compaction process could be a sedimentation, centrifugation, filtration, or slip casting as in ceramics, or tableting as in pharmaceuticals, or pressure injection molding. Other processes for producing thin solid films involve deposition in large thermal gradients and splat quenching on to a colder substrate.

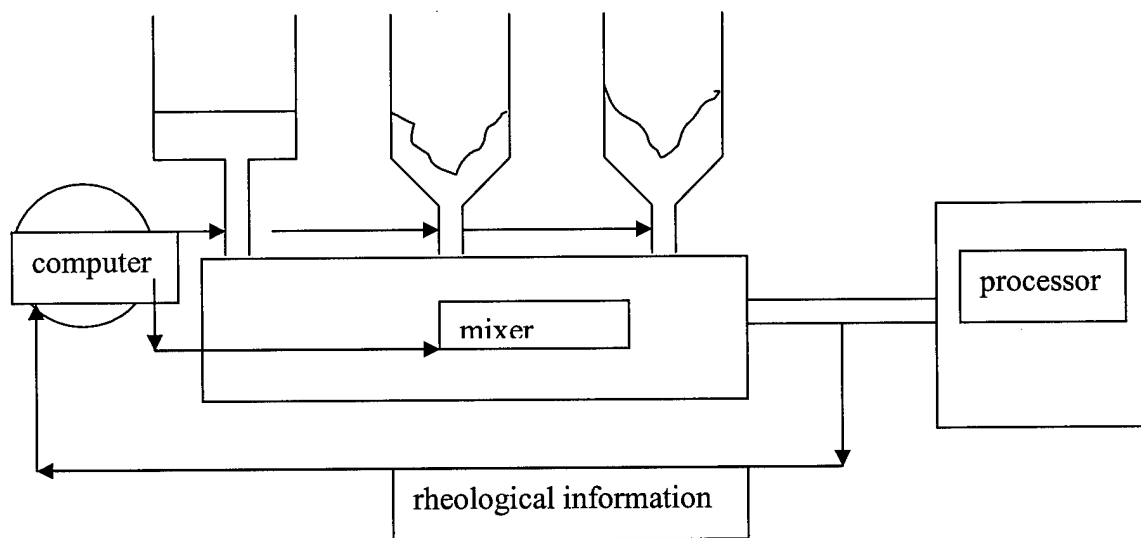


Figure 1 : Schematic chart of a typical production process for a binary composite material processed continuously via a colloidal suspension.

The shear flow and deformation processes that determine the final product require a prediction of the fluid mechanics of the mixed suspension [2] The rate of flow and the distribution of particulates as a function of flow rate, i.e. the fluid mechanics of the colloidal suspension in a given geometry is crucially dependent of the solid fractions of the two powders and their variable particle size distributions, and on the viscosity and temperature of the liquid. Control of the composition of the feeds and the liquid flow therefore requires feedback information of the constitutive rheological relations that will enable computational fluid mechanics of the suspension after mixing and during processing.

When a colloidal suspension is subjected to any stress deformation, the osmotic thermodynamic and transport properties of the particles themselves become a function of deformation rate, in addition to the stress. Finite element and finite difference CFD simulations of particulate systems require the osmotic pressure, the particle diffusivity, and the particle kinetic energy conductivity, all as a function of the rate of deformation.

In principle there are three possible ways to obtain all or part of this information. The conventional chemical engineering approach, either batch-sample or on-line, is to measure the "flow curve" of the suspension, i.e. the stress as a function of concentrations, and the rate of shear strain, concentrations and temperature, and to utilize that information. This approach is intrusive and fraught with problems. Under shear flow the particles reorganize themselves to minimize the stresses. Rheometric viscosity data for dense suspensions are geometry dependent, and are neither scalable nor transferable from one rheometric or processing device to another [2,3] Elongational viscosities are impossible to access experimentally.

An alternative approach is to obtain all the requisite details of the particle size and shape distributions, the liquid medium density and viscosity, etc., and to utilize the methods of computational statistical mechanics. In principle, given the essential information, mesoscale modeling will eventually be able to make *ab initio* predictions of the fluid mechanics of complex suspensions, but there is a long way to go. The programs, which have been developed here for compaction processes, can be regarded as a preliminary step along the path to an integrated computational rheometry of colloidal systems.

In recent years there have been developments in non-intrusive methods that gather data by various means, and utilize that advances in computing to reconstruct a detailed picture of the interior. These methods are also promising to obtain information on the concentration of

particles and velocities of particles during shear flow and processing and, potentially, can yield the necessary constitutive rheological relations, by on line techniques. One such method is the use of Raman spectra tomography, which is being pioneered in the Materials Directorate AFRL in Dayton. A second and subsidiary objective in this project is to test a literature method for the production of a prototype monodisperse latex, with the particle diameter of the wavelength of green light (532nm), in laboratory experiments.

2) Mesoscale model

The simulation of colloidal particle motions by methods akin to Monte Carlo and molecular dynamics of computational statistical mechanics have come to be known as mesoscale modeling [4]. Both granular dynamics simulations of inelastic particles, and Stokesian dynamics simulations of particles in hydrodynamic media are more akin to NEMD (non-equilibrium molecular dynamics) in that there is no inherent thermodynamic equilibrium. In the simulation of flows and deformations of colloidal systems, the particle movements are driven by externally imposed forces.

If we have sufficient knowledge of the interparticle forces, and other essential particle characteristics, such as polydispersity of size and shape, surface charge and friction effects etc. in principle the entire constitutive rheological relations that are required for fluid mechanics predictions in given geometries can be obtained. "Computational rheometry" is still in very early stages. In principle it is possible because the two major obstacles to obtaining experimental flow curves via conventional rheometry can be eliminated in idealized computer experiments.

The general methodology that has been employed is classical molecular dynamics in which the equations-of-motion of large numbers of particles are solved simultaneously. These could be macromolecules, nano-clusters, colloidal particles in suspension, or inelastic granular particles which dissipate energy on collision. The interparticle forces vary with model material. The equations of motion can be readily changed from Newtonian, to granular with inelastic interactions, or Stokesian/Brownian for suspensions.

In the present preliminary investigation of continuous thin-film solidification, the equations of motion have been so far restricted to classical [Newtonian].

Sliding-brick periodic boundaries [5]

The computational tricks are first to eliminate the presence of driving surfaces by periodic boundary conditions and then, secondly, to impose a uniform homogeneous shear field by velocity scaling methods. Both these conditions enable the simulation of truly homogeneous shear flow regimes with the system steady-state variables prescribed. It should be noted the homogeneous shear steady-state computations have no real experimental counterpart. In principle, however, these simulations will lead to the computation of the constitutive rheological relations for the model material. This information, in turn, will enable CFD (computational fluid dynamics) predictions for colloidal fluids in processing geometries.

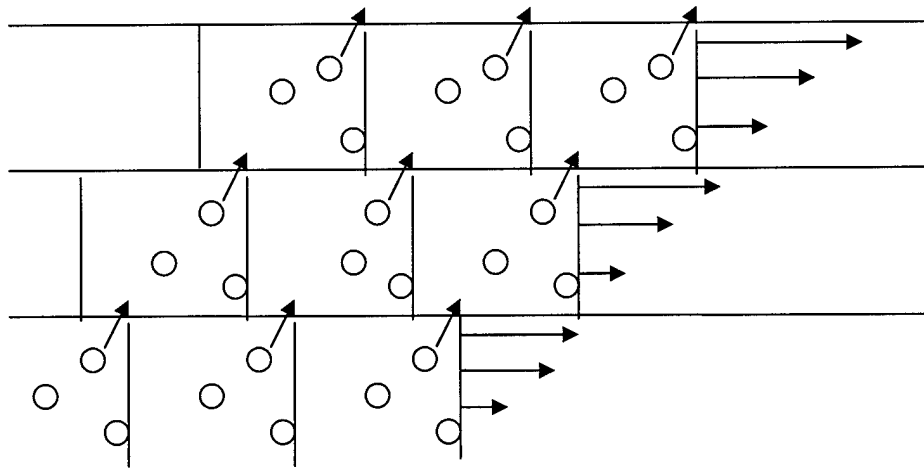


Figure 2 : Periodic boundaries for simulation of steady-state homogeneous flow of a particulate suspension; both the linear velocity gradient and the concentration remain uniform.

Uniaxial compaction periodic boundaries [6]

Periodic boundary conditions have also been devised for continuous elongational and compressive deformations and these enable the computation of non-linear elongational properties of particulate systems. These boundary conditions can be generalized to a whole range of uniaxial compaction processes and in principle can be used to simulate the processes referred

to in the introduction for the production of binary composite solids for example. Hence, the constitutive rheological relations for the solidification processes for colloids can, in principle, be predicted computationally.

boundary
velocity (v_b)

driving
force (F_d)

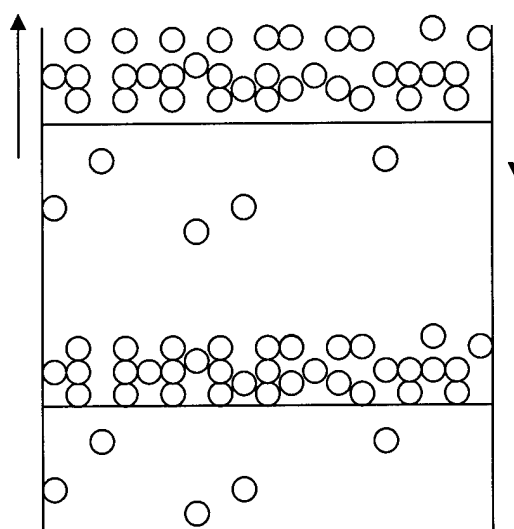


Figure 3 : Periodic uniaxial compaction boundaries; under certain conditions of the prescribed driving force and interface velocity, this system exhibits two-phase behavior as described in the text. The pressures and diffusivities of the “feed” and the “bed” phases, as a function of the driving force (F_d) and the rate constant (v_b), are required for CFD simulations of the corresponding batch processes.

When an external force, such as a gravitational field, is applied to a dynamical system, if the boundary in the direction of the force is rigid, the particles will condense and a time-dependent process will lead to a batch solid film at that boundary. If, on the other hand, the boundary is periodic, the particles will eventually just move in a steady state through the system, from one side to the other, recycling, with no change in properties. When a semi-permeable hybrid boundary is used however, a steady-state uniaxial compaction process is effected in which a low density “feed” phase moving with a high mass velocity moves continuously in coexistence

with a high-density solid material phase moving with a lower mass velocity (to maintain the mass and force balance), and an interface between them.

Processes that do not characterize the solid state generally produce non-crystalline solid materials. For example, solids produced by industrial crystallization or precipitation are processed by uniaxial compactions, such as sedimentation, filtration, or centrifugation. Because of the change in conditions at the deposition interface with time in these batch processes (the driving force usually weakens with time), an inhomogeneous bulk solid-state material is produced that cannot be characterized. This implies that problems will be encountered in defect and grain boundary inhomogeneities, non-reproducibility and quality control.

These imperfections cannot be tolerated in many modern materials. If it were somehow possible to devise well-characterized steady-state processes that continuously produce advanced solid composite materials such as carbon composites, ceramics etc., it might eventually be possible to uniquely characterize these advanced solid materials by just one (if gravity is fixed) or possible two additional state variables that describe the process that produces the non-equilibrium solid.

The unique characterization of non-equilibrium solid materials by the thermodynamic conditions at which they exist (temperature and either pressure or density), and the process that produces them puts the characterization of the state of advanced materials a sounder scientific base. Equation-of-state, transport coefficients, and other constitutive properties could be raised to a status of reproducibility to that of equilibrium fluids and some equilibrium well-characterized crystalline materials. A complete control model of these idealized material production processes is then possible. In the following section, the idealized process of uniaxial compaction is investigated in a system of steady-state conditions using simulation programs that have been developed as a part of this project.

In the case of solids produced from granular materials, powders, suspensions of powders and other colloidal particles, the state of the feed materials must also be addressed, as colloids are generally difficult to characterize. Below we develop a program for simulating the continuous production of a high density solid phase continuously in steady-state equilibrium with a low density feed phase. The determination of the properties of these materials by computational statistical mechanics methods at the colloidal particulate level is the immediate priority of the present project.

3) Simulations

In all the programs used and developed for this project to date, (see APPENDIX 1) the 6N coupled first-order differential equations of classical particle motion are

$$d\mathbf{r}_i/dt = \mathbf{v}_i$$

and

$$d\mathbf{v}_i/dt = \mathbf{F}_i / m_i$$

Simple one-step predictor methods are adequate. In a finite difference form

$$d^2\mathbf{r}_i/dt^2 = \mathbf{F}_i(t) / m_i = \{[\mathbf{r}_i(t+dt) - \mathbf{r}_i(t)] - [\mathbf{r}_i(t) - \mathbf{r}_i(t-dt)]\}/dt^2 + Odt^4$$

where dt denotes the time step in the numerical integration. The simple algorithm is then

$$\mathbf{r}_i(t+dt) = 2 \mathbf{r}_i(t) - \mathbf{r}_i(t-dt) + dt^2 \mathbf{F}_i(t) / m_i + Odt^4$$

The algorithm can be made self-starting if the initial velocities are specified and used to define

$$\mathbf{r}_i(t-dt) \text{ and specify at } t=0 \text{ i.e. } \mathbf{r}_i(t-dt) = \mathbf{r}_i(t) - \mathbf{v}_i(dt=0) / dt$$

then the algorithm for position and velocities respectively are

$$\mathbf{r}_i(t+dt) = \mathbf{r}_i(t) + dt \mathbf{v}_i(t) + dt^2 \mathbf{F}_i(t) / m_i + Odt^4$$

$$\mathbf{v}_i(t+dt) = \mathbf{v}_i(t) + dt \mathbf{F}_i(t) / m_i$$

The whole system is divided up into cells, nlx, nly and nlz being the total number of neighborhood compartments in each dimension. The total number of cells is NLX x NLY x NLZ. The particles are then indexed in order of position beginning with the first particle in cell 1, and keeping a track of the number of particles in each cell. As the particles move around the system, their indices change. The code for updating the indices is much faster than conventional LINK cell methods and may be more amenable to parallelization. (see APPENDIX 1)

a) MNCELL.f

A computer program has been developed as an extension of the previous program (referred to as LJLINK.f), for a system of three dimensional particles that was used to explore the phase behavior and continuous production of an amorphous solid of n=12 soft spheres by Warr and Woodcock [6]. The program requires 3 basic ingredients over and above a classical 3D homogeneous MD program [4]

System (model) : interparticle forces for colloidal particles in the first approximation have two components, a steep positive repulsion clouds overlap at short-range, and a longer range negative attraction which decrease with an inverse power (1-6) of the distance. Here a more general form of the Lennard-Jones pair potential, m-n potential, in which the minimum distance (r_0) is used, rather than the collision distance of zero potential.

$$E_o = \sum_{\text{non-bonded particles}} \epsilon_{AB} \{ (r_{oAB}/r)^n - 2(r_{oAB}/r)^m \}$$

The m-n pair potential contains only two-parameters the energy at the minimum ($-\epsilon$) and the minimum energy distance (r_0) when the force is zero: n determines the "hardness" of the potential and m determines the "range" of the attraction.

For binary systems the *Lorentz-Berthelot rules* for determining the parameters, that were originally applied to mixtures of rare gas atoms are used

$$\epsilon_{AB} = (\epsilon_{AA}\epsilon_{BB})^{1/2} \quad \text{and} \quad r_{oAB} = \frac{1}{2} (r_{oAA} + r_{oBB})$$

For ionic systems *Coulombic potentials* the charge distribution can be represented by a set of two or more point charges, usually, but not necessarily, centered on the particle, but in any case fixed relative to the particle in space. The total Coulombic potential is then

$E_c = \sum_{ij \text{ charge pairs}} Z_i Z_j e^2 / r_{ij}$ where Z_i and Z_j are the charges in dimensions of the charge of an electron (e). The programs developed are general but all the test runs to date refer to an m-n single component fluid n=12 and m=6.

System-state variables: cell dimensions, density, temperature

For a fully periodic system, once the size and shape is specified (in the three side length variables XF YF ZF with XF =1 the dimension of length used in the program.

$$\text{Volume} = XF \times YF \times ZF$$

The number of particles N is fixed

$$\text{Mean density } \rho = N/V$$

$$\text{Kinetic energy} = \sum m v^2$$

$$\text{External driving force} = Fd$$

$$\text{Boundary velocity} = Vb$$

All the variables are in m-n pair potential dimensionless reduced units.

It is the two steady-state variables that conspire to create in certain regions of parameter space a two-phase solidifying system of a low density phase moving with a high velocity (feed

phase) in coexistence with a high density solid phase moving with a low velocity with and interface.

Boundary conditions:

For the test program MNCCELL there is full periodicity in both of the directions perpendicular to flow, i.e. X periodic Y periodic Z semi-permeable (finite Vb)

A sequence of test runs on the USAFR Computational facility Orion (acomputerforme.com) at San Antonio have been carried out. The full Output are on file as labeled in table 1 below.

TABLE 1: Test runs for MNCCELL $\rho = \rho_0^3/V = 1.0000/ T = 1.0000$; cubic

Run/OP	N	Time/dt	Fd	Vb	<U>	<p>	Comments
MNOP1	2048	100000	10.0	0.1	-2.277	30.21	2-phase/gas-cryst/sharp
MNOP2	2048	40000	10.0	0.01	-2.330	31.04	perfect crystal/zero flux
MNOP3	6912	100000	1.0	1.0	-4.019	2.67	2-phase/ dense fl. am..sol
MNOP4	8788	100000	10.0	0.05	-0.878	38.21	Equilibration run/slow
MNOP5	8788	1000000	10.0	0.05	-0.716	43.36	2-phase/gas-cryst/sharp
MNOP6	8788	1000000	1.0	0.05	-4.488	6.173	2-phase/gas-cryst/ diffuse
MNOP7	8788	1000000	1.0	0.05	-4.493	6.143	2-phase/gas-cryst/sharper
MNOP8	8788	1000000	1.0	0.05	-4.286	6.235	2-phase/gas-cryst/sharp

At high velocities (>1) and low driving force (<1) a single amorphous phase is obtained, but the table above shows that there is a wide range of parameter space that leads to a continuous solidification, with a low density feed, an interface, and a high density solid. The solid may be crystalline, amorphous or possible metastable.

Run 3 (Vb=1,Fd=1) is 2-phase but close to the one phase boundary.

For all the runs profiles in the heterogeneous Z-direction (i.e. the direction of flow) are accumulated. A typical set of profiles for a steady-state system showing two phases with crystallization is given in Table 2 below.

TABLE 2: EXAMPLE of 2-phase PROFILES for TEST RUN 1

The profiles are. Respectively, index of bin, height Z (if force is gravity), density(ρ), velocity in z-direction (of flow), mass flow rate (flux), kinetic energy (KE), potential energy (PE), and interfacial stress for each layer ($-P_{xy}$)z.

h	Z/ro	RHO	VZ	<flux>	KE	PE	STRESS
50	12.45	0.013	-1.811	-0.024	2.379	-3.758	-0.087
49	12.19	0.013	-1.947	-0.025	2.702	-4.416	-0.024
48	11.94	0.017	-1.530	-0.027	2.066	-4.013	-0.011
47	11.68	0.025	-1.097	-0.028	1.607	-3.439	-0.050
46	11.43	0.028	-1.043	-0.029	1.658	-2.800	-0.067
45	11.18	0.024	-1.283	-0.030	1.927	-2.621	-0.033
44	10.92	0.023	-1.377	-0.032	2.000	-2.675	-0.018
43	10.67	0.023	-1.420	-0.033	2.019	-2.736	-0.022
42	10.41	0.023	-1.457	-0.034	2.072	-2.773	-0.016
41	10.16	0.025	-1.441	-0.035	2.139	-2.891	-0.015
40	9.91	0.025	-1.460	-0.037	2.178	-3.004	-0.010
39	9.65	0.026	-1.472	-0.038	2.210	-3.097	-0.011
38	9.40	0.027	-1.469	-0.039	2.195	-3.213	-0.010
37	9.14	0.027	-1.503	-0.041	2.194	-3.328	-0.012
36	8.89	0.028	-1.480	-0.042	2.131	-3.403	-0.008
35	8.64	0.029	-1.475	-0.043	2.145	-3.476	-0.014
34	8.38	0.030	-1.499	-0.044	2.209	-3.554	-0.011
33	8.13	0.031	-1.484	-0.045	2.143	-3.796	-0.011
32	7.87	0.031	-1.488	-0.047	2.157	-3.862	-0.011
31	7.62	0.034	-1.430	-0.048	2.104	-3.907	-0.002
30	7.37	0.038	-1.308	-0.049	2.010	-3.842	0.007
29	7.11	0.068	-0.738	-0.050	1.597	-3.316	0.020
28	6.86	0.410	-0.118	-0.048	1.106	-3.137	0.086
27	6.60	1.539	-0.033	-0.051	1.020	-3.605	3.929
26	6.35	0.518	-0.105	-0.054	1.042	-4.013	0.692
25	6.10	0.865	-0.054	-0.047	1.021	-4.986	-2.228
24	5.84	2.896	-0.017	-0.050	0.991	-5.145	-1.371
23	5.59	0.528	-0.106	-0.056	0.995	-5.176	0.419
22	5.33	0.723	-0.062	-0.044	0.994	-5.838	-1.736
21	5.08	3.636	-0.014	-0.052	0.982	-5.363	-14.090
20	4.83	0.325	-0.155	-0.050	0.927	-5.298	-0.201
19	4.57	0.842	-0.046	-0.039	0.967	-5.845	-1.149
18	4.32	3.701	-0.015	-0.056	0.977	-5.169	-17.902
17	4.06	0.273	-0.163	-0.044	0.852	-5.209	0.160
16	3.81	2.319	-0.005	-0.012	0.977	-5.073	-10.525
15	3.56	2.260	-0.034	-0.077	0.982	-4.674	-11.028
14	3.30	0.320	-0.131	-0.042	0.837	-4.523	-0.063
13	3.05	4.096	-0.010	-0.039	1.025	-4.690	-16.131
12	2.79	0.252	-0.168	-0.042	0.843	-4.258	-0.375
11	2.54	0.823	-0.025	-0.020	0.935	-4.017	-1.515
10	2.29	3.849	-0.015	-0.057	0.980	-4.034	-4.991
9	2.03	0.252	-0.143	-0.036	0.827	-3.747	0.447
8	1.78	4.096	-0.008	-0.031	1.042	-3.509	3.837
7	1.52	0.230	-0.169	-0.039	0.951	-3.236	-0.787
6	1.27	0.879	-0.010	-0.009	0.952	-2.440	1.998
5	1.02	3.828	-0.015	-0.057	0.987	-2.354	12.101
4	0.76	0.134	-0.225	-0.030	1.006	-4.123	-0.495
3	0.51	4.096	-0.007	-0.030	1.091	-1.324	32.627
2	0.25	0.059	-0.473	-0.028	1.168	-2.813	-0.365
1	0.00	4.096	0.112	0.458	1.053	-1.659	-25.570

b) MNSLAB.f (see appendix I)

A derivative computer program has been developed in which the periodic boundaries in the Y-direction are made to be rigidly reflecting rather than periodic. The program simulates the continuous production of a thin solid film in which the particles are constrained to move between the two boundaries.

The system and system-state parameters are the same as MNCELL above, but the system is not periodic in one of the perpendicular directions (Y). The periodic boundary conditions in the Y-direction are replaced with rigid reflecting container walls.

Although, for testing purposes, the boundary conditions in the direction of uniaxial flow (Z) remain as in MNCELL above, we note at this stage that one of the rigid boundaries in the direction perpendicular to the slab can be removed such that in the presence of a second perpendicular external force (e.g gravity) or an adhesive. Under these conditions open surfaces can be used for thin film production. In this way, the program can be easily modified to simulate a real process of laying down a continuous solid tape, under gravity, on an adhesive substrate.

The results for a set of test runs for the program MNSLAB with $n=12$ and $m=6$, and density and kinetic energy ("temperature") set equal to 1 as above, are summarized in Table 3 below.

TABLE 3: Test runs for MNSLAB $\rho=Nr_o^3/V=1.0/ T=1.0$; slab/rigid Y

Run/OP file	N	Time/dt	Fd	Vb	<U>	<p>	Comments
MNOPSL1	1024	100000	10.0	0.05	-3.169	1.574	1x0.125x4 Equilibration
MNOPSL2	1024	1000000	10.0	0.02	-3.235	53.12	2-phase/order solid
MNOPSL3	1024	1000000	10.0	0.5	-3.415	1.269	1-phase amorphous
MNOPSL4	1024	100000	10.0	0.1	-3.174	1.529	1-phase amorphous
MNOPSL5	1024	100000	10.0	0.02	2.339	45.33	2-phase amorphous sol.
MNOPSL6	1024	1000000	10.0	0.02	3.392	54.24	vac/cryst zero flow
MNOPSL7	1024	1000000	10.0	0.01	9.730	79.62	Eq.1x0.625x8 2-phase cryst
MNOPSL8	1024	1000000	1.0	0.01	-2.429	12.06	" vac/cryst(1.64) zero flow
MNOPSL9	1024	1000000	1.0	0.02	-2.393	12.32	" vac/cryst(1.64) zero flow

MNOPSL10	1024	1000000	0.5	0.2	-2.849	6.602	“ gas(0.012)/cryst(1.64)
MNOPSL11	1024	1000000	1.0	0.1	-2.427	11.35	“ gas(0.001)/cryst(1.64)
MNOPSL12	1024	1000000	0.5	0.4	-2.939	6.098	“ gas(~0.065)/ cryst(0.33)

The results show that the same pattern of 2-phase behavior can be obtained for the full periodic system. At very low velocities the system crystallizes completely such that there is no perceptible feed phase, i.e. it appears to be a vacuum. There appears to be a fairly narrow range of 2-phase behavior, when $F_d=10$, because for $v_b > 0.1$, only a single amorphous phase is obtained. It is clear that the phase behavior depends strongly on the dimensions of the slab. For a different shaped slab, which is only half as thin (Runs 6-12), the results are quite different.

c) IONCELL.f

A third modification program has been developed which can be used for binary systems and ionic systems, in this case the pair potential takes the form ($m=1$)

$$E_o = \sum_{\text{non-bonded particles}} \epsilon_{AB} \{ (r_{oAB}/r)^n - 2Z_i Z_j (r_{oAB}/r) \}$$

the program has been modified and placed on Orion ready to be tested both for full periodicity, and thin film production, for an ionic salt such as the solidification of sodium chloride.

4) Colloidal rheometry

Computational fluid mechanics requires just two ingredients (i) solution of the conservation equations of continuum motion, and (ii) constitutive rheological relations for the material constituent fluids properties. The latter are unknown and inaccessible for complex colloidal fluids, such as powders, suspensions of powders, plastisols and bio-fluids e.g. blood. Conventional rheometry, that senses stress or strain rate at driving surfaces, cannot detect the spatial variations in velocity gradients and particle concentration caused by the shear field.

As demonstrated already in these computations, in principle, the obstacles of conventional rheometry can be eliminated with the use of surface-free periodic boundaries and the imposition of linear profiles artificial “thermostatting”. The situation at present, however, is that we are still someway from obtaining the overall constitutive rheological relations that will

enable flow prediction of real colloidal suspension. Also, progress is hampered due to a lack of requisite quantitative information of the interparticulate forces.

Very recently, new non-intrusive experimental methods are being researched and developed. that can sense the velocity gradients, and flow profiles, and hence access the stresses, and the constitutive rheological properties of complex non-Newtonian fluids in flow. Such techniques as laser Doppler anemometry, NMR tomography, positron tracking (for doped systems). All these methods have inherent disadvantages. A new, promising technique at an early stage of development which is non-intrusive, relatively inexpensive and fast, uses Raman light scattering.

The problems with conventional rheometry for suspensions can be summarized as follows. The thermodynamic state of the suspension is itself a function of the rate of deformation; it is this aspect, the lack of knowledge or information of the change in osmotic state and particle transport properties with deformation rate, that renders conventional rheometry inapplicable.

Consider a particulate fluid in steady shear flow in a typical rheometer. When steady-state is reached there are forces at play that make the particulate system inhomogeneous. It follows that the rheological information that is obtained is peculiar to the geometry of the flow device. The three most common such devices are the coaxial cylinder, the cone-and plate and the capillary rheometer.

When a colloidal suspension is at rest the particles can come to equilibrium via Brownian motion, and they exhibit osmotic properties of classical thermodynamics. Osmotic pressures of suspensions of colloidal particles, of-the-order 1 micron or larger, are very small [ca 10^{-4} atm. at $\phi = 50\%$ solids]. When a system of colloidal micro-particles, however, is subjected to shear flow, the hydrodynamic forces on the particle cause drastic increases in osmotic pressure with the square of shear gradient. At extreme rates of shear, for example in very fast roll coating operations, the osmotic pressure can exceed one atmosphere causing an apparent surface drying effect, which is a well known phenomenon for "dilatant" dense suspensions, and has to be avoided by working at shear rates lower than the critical shear rate for dilatancy.

As a consequence of the above effects, dense suspensions can become inhomogeneous during flow and processing; the particles tend to migrate from regions of high shear to regions of low shear. The net result of this readjustment in the three rheometers above is spurious

rheological data, because of the incorrect assumption of homogeneity. In the co-axial cylinder the particles move away from the driving surface and towards the immobile surface (the cup). In the cone and plate the particles can cake on the plate, and the effect in the case of the capillary rheometer is that particles move from the pipe wall, where the shear rate is greatest towards the pipe axis where the shear rate is zero. In an extreme case of the latter "plug" flow results. This effect in a capillary rheometer would cause the apparent shear viscosity to appear to be much lower than it would be for the homogeneous suspension.

All these undesirable effects can also occur in transport and processing devices and need to be predicted and controlled.

Not only is the composition of the suspension in shear flow rheometers inhomogeneous, but so also is the shear gradient. Under inhomogeneous conditions the system further adjusts to a high velocity gradient where the viscosity is low, in regions of low concentration, and a low gradient, or flow rate, in regions of high concentration. The extreme consequence of the above inhomogeneities in concentration and shear gradient is a problem well-known to chemical engineers, accumulation and "caking" of the particles in a static region of zero flow.

It follows that the constitutive rheological relationships for the effect of a shear flow field on the stresses, not just the non-Newtonian viscosity, but also osmotic pressures and particle diffusivities of colloidal suspensions, are inaccessible by conventional rheometric devices.

On the experimental side, the use of conventional rheometry for particulate systems is now accepted to be untrustworthy. Real progress towards accurate, though perhaps, more limited, rheological properties, is now being made with the development of powerful non-intrusive experimental techniques for obtaining rheological information from suspension flow. All have inherent advantages and disadvantages regarding cost, sample requirements, and accessibility. Eventually, it is hoped that a relatively simple cost-effective technique will emerge, perhaps the Ramascope for particles that it can "see" is the most promising but it is at the earliest stage of development.

It is to facilitate the development of this non-intrusive technique that a standard crystallizable monodisperse colloid that is reproducible is required. To this end, we have explored a recent experimental prescription [8,9] that promised to synthesize, to size order, samples of monodisperse latex with neutral surfaces (hard-spheres) that suspend in water with neutral buoyancy.

5) Monodisperse submicron latex: experimental synthesis

Starting from the work in 1982 of Almog and co-workers [7] on the production of spheres by a single-step dispersion polymerization process. The simplicity of this process was a factor in its popularity for study and variations were made including varying the monomer, studying the roughness of the particles where the properties of the steric stabilizer were investigated, and investigating the deformability of particles where cross linked spheres were produced without stabilizers. The mechanism of dispersion polymerization is more complex and remains less well understood than emulsion polymerization. As a consequence of this ignorance It has been difficult, until recently, to prepare submicron monodisperse latex, to a prescribed particle diameter and sharp monodispersity.

To produce particles in the sub-micron range, micro-emulsion polymerization is used. A two-stage process, micro-emulsion preparation and then polymerization usually achieve this. In this system it is accepted that the principle loci of polymerization are the monomer swollen latex particles. However the particles produced by this method exhibited a wide size distribution skewed to the smaller size range. Thus if a narrow size range is desired it is necessary to shorten the nucleation period and avoid homogeneous nucleation in the aqueous phase. Using a redox initiator system, with a faster dissociation rate than a thermal system lowers the nucleation period [reference 8 papers 79,80] this has been coupled with the use of a saw-toothed blade mixer for improved agitation. Particles produced by this method have a very narrow distribution and a size range of 100-150 nm. We require particles around the 500nm range.

Conventional surfactants are small and mobile and can migrate to the surface layer of a polymeric film. This can have a negative effect on the application properties. One solution is to use a polymerizable non-ionic surfactant which can be incorporated into the particles during polymerization as described by Chern et al. (1996) [reference 8 paper 81].

Turning now to the very specific objective of producing idealized hard-sphere particles with the three requirements of sharp monodispersity, a prescribed particle diameter and possible scale-up requirement. Polystyrene latex produced by dispersion polymerization using the very recent technique developed in the last 3 years in references [reference 8 papers 83-85]

The use of polyethylene oxides by Lin and co-workers 1999 gave polystyrene particles of average size 300 nm. Liu and coworkers 1997 and 1998 have used the same class of stabilizers in dispersion polymerization of styrene to give particles in the range 100 nm to 1 micron. Production of particles "to order" at a prescribed diameter therefore now seems practicable subject only to some preliminary R&D work. The effect of scale-up is unpredictable at this stage and needs to be researched.

The currently achievable standard deviations of the particle size distribution is about 1 %. Thus it should be possible, without too much difficulty, to produce kilogram quantities (at least) of hard-sphere PS in the size range 530-535nm in the near future if need be.

EXPERIMENT: METHOD of Liu et al. (1998)

Previously using the Almog method monodisperse polymeric spheres in the micron size range were produced in one step. These have already been supplied to the Materials Research Directorate at AFRL [7,8] Now, a new method will be used to produce monodisperse polymeric spheres in the nanometer size range. This method involves the dispersion polymerization of styrene with a small amount of the polymerizable w-methoxy poly-ethylene oxide undecyl-a-macro-monomer (PEO-R-MA-40) as the stabilizer.

We have followed the prescription of Liu et al. (1997). This is based on the dispersion polymerization of styrene using a small amount of macromonomer (PEO-R-MA-40) in ethanol-water media.

According to Liu et al. the resultant size can be formulated. The mean diameter of the latex particles obtained is given by a simple formula that depends on the relative mass fractions of stabilizer (PEO-R-MA-40), surfactant (AIBN), and styrene, at the outset of the polymerization as follows.

$$D \times CF^3 = [\text{PEO-R-MA-40}]^{-0.6} [\text{styrene}]^{1.02} [\text{AIBN}]^{-0.09}$$

Where D is the requisite mean particle diameter and CF is the fractional conversion of the monomer styrene to polymer. In the first reproducibility test of the above the [styrene] and surfactant [AIBN] are fixed and [[PEO-R-MA-40] varied such that when the polymerization is stopped at a given conversion, particles of size less than 500nm are obtained.

The first phase of this work is completed, and has been concerned with the synthesis of the macromonomer (PEO-R-MA-40), this has successfully been done following the prescription given by Liu et al. This is being used together with styrene in the second phase of the work to produce monodisperse spheres. The method of Liu et al has now been successfully reproduced to produce particles in that size range. The first product showed sub 500nm particles with rather a wider polydispersity than expected, but the samples have not yet been fully analyzed for size distribution except under a microscope. This research is continuing. A list of all the reagents that we have had to procure in order to synthesize 500nm latex by this method is summarized in the appendix spheres will be available and analyzed before 28/02/01.

In summary we now have the facility to produce small laboratory scale quantities of monodisperse aqueous latex with a mean particle size distribution of the same range as the visible spectrum of light. At this stage it is not possible to say just how precisely a particular color e.g green 532 ± 5 , say, can be targeted.

To date we have found no literature or published attempts to scale up beyond the laboratory scale of less than Order 1kg, i.e. to produce commercial quantities. The research papers of Liu et al., as with previous papers on laboratory dispersion polymerization, give no information on the effect of scale up on their formula that holds for sub-kilogram quantities on the 1litre laboratory batch scale.

REFERENCES

- [1] These programs have been developed from a program LJLINK.f that uses conventional LINK-CELL methods of neighborhood listings that were developed by the reporter in the 1970's and are described in numerous places in the UK CCP5 Molecular Simulation Quarterly Newsletter. The original LJLINK.f program is available from L V Woodcock.
- [2] Johma, A.I., Merrington, A., Woodcock, L.V., Barnes H.A., Lips A., Powder Technology **65**, 343-370 (1991)
- [3] Woodcock, L.V., "Osmotic pressure effects in dispersion rheometry", J. non-Newtonian Fluid Mechanics, **19**, 349-355 (1986)

[4] Nicolaides, D.B. (Molecular Simulation Corp.) Editor, "Meso-scale Modeling", (Cambridge: in the press)

[5] Lees, A. and Edwards, S.F., "The viscosity of liquids under extreme conditions", J. Physics C 5 1921 (1972)

[6] Warr, S., and Woodcock, L.V. "Solid-fluid interfaces in non-linear steady states", J. Chem. Soc. Faraday Discussion 95, 325-346 (1993)

[7] Bradley, J., "A study of the feasibility of using Raman Spectroscopy to Probe the structure and intermolecular forces of mesoscopic matter", M. Eng. Dissertation (research carried out at AFRL) University of Bradford (2000)

[8] AFRL Report "The synthesis of monodisperse submicron solids; prospects for advanced materials processing", Overview and Literature Survey, L. V. Woodcock, Scientific Simulation Services (July 2000)

[9] Liu, J., Chew, C.H., Wong, S. Y., Lin, J. and Gan, L.M., "The particle size of latexes from dispersion polymerization of styrene using polyethyleneoxide macromonomer as a polymerizable", J. Polymer Science Part A Polymer Chem. 35, 3575-3583 (1998)

[10] Liu, J., Chew, C.H., Wong, S. Y., Gan, L.M., Lin, J. And Tan, K. L. , "Dispersion polymerization of styrene in aqueous ethanol media using polyethyleneoxide macromonomer as a polymerizable stabilizer", Polymer 39, 283-289 (1998)

APPENDIX 1 MNSLAB.f annotated

```

PROGRAM MNSLAB
C MNSLAB LAST REVISION 17 NOV 00
  DIMENSION RX(12000), RY(12000), RZ(12000)      particle positions
  DIMENSION VX(12000), VY(12000), VZ(12000)      particle velocities
  DIMENSION FX(12000), FY(12000), FZ(12000)      particle forces
  DIMENSION PZZ(12000), PS(12000), SZ(12000)      particle pressures and stresses
  DIMENSION DISPX(12000), DISPY(12000), DISPZ(12000) particle displacements
  DIMENSION X0(6), Y0(6), Z0(6)                  initial lattice coordinates (4 for fcc cell)
  DIMENSION NIN(8000), L0(8000), L1(8000)         no. of particles, first and last in n-th cell
  DIMENSION DEN(200), VLZ(200), TEE(200), STR(200), POT(200), ZZZ(200) Z-profiles of density, velocity, kinetic
                                                    energy, stress, potential energy and
                                                    pressure pzz

  DIMENSION DXSQ(12), DYSQ(12), DZSQ(12)          mean-square displacement by layer
  DIMENSION TEELAY(12), POTLAY(12), STRLAY(12)     KE, PE and stress by layer
  DIMENSION XNORM(12), XSUM(12)                   accumulators of layer number densities

C
  OPEN(5, FILE='MNDATA')      input data parameters
  OPEN(6, FILE='MNRES')       print out results
  OPEN(7, FILE='MN1024')      configuration of positions and velocities/start/end

C
C PAIR POTENTIAL              PHI = Ar**(-m) + Br**(-n)
C PARAMETERS
  READ(5, 100) N, M, CO       attractive and repulsive exponents, cut-off in units of r0
100  FORMAT(2I3, F5.2)
  A = FLOAT(N)/FLOAT(M - N)
  B = FLOAT(M)/FLOAT(N - M)
  WRITE(6, 200) N, M, A, B, CO
  M2 = M/2
  N2 = N/2

C
C SYSTEM STATE
  READ(5, 101) RHO, TI        system density and initial temperature
101  FORMAT(2F8.4)
C STEADY STATE PROCESS VARIABLES
  READ(5, 102) FDZ, VBZ, NVB  system driving force, boundary velocity (compaction velocity), NVB is z-boundary
conditioin
102  FORMAT(2F8.4, I3)
  IF(NVB.EQ.1) WRITE(6, 221)
  IF(NVB.EQ.2) WRITE(6, 222)
  IF(NVB.EQ.3) WRITE(6, 223)

C
  WRITE (6, 201) RHO, TI, FDZ, VBZ

C
C PROGRAM CONSTANTS
  READ(5, 103) NA             total number of particles
103  FORMAT(I8)
  WRITE (6, 202) NA
  XNA=NA
  READ(5, 104) NRUN           index of run 0,1,2,3,etc. lattice start for run0
104  FORMAT(I3)
  READ(5, 105) NDT, DT, ISCALE number of time steps, time increment, thermostat or not (0 or 1)
105  FORMAT( I8, F8.4, I3)
C PRINT FREQUENCY
  READ(5, 106) NSUB
106  FORMAT(I8)
  XNSUB = NSUB
  WRITE (6, 203) NRUN, NDT, NSUB, DT, ISCALE

C
C BOX SHAPE DIMENSIONS        volume in reduced units XF x YF x ZF

```

```

      XF = 1.0
      READ(5,107)YF,ZF
107  FORMAT(2F8.4)
      WRITE(6,206)XF,YF,ZF
C
C CONVERSIONS TO PROGRAM UNITS
C LENGTH is length of box in X, MASS is particle mass, and TIME is DT
      XL=(XNA/(RHO*YF*ZF))**(1.0/3.0)
      R0 = XF/XL           distance of minimum potential in program units
      EPS=R0*R0*DT*DT      minimum pair energy in program units
      A=A*EPS*(R0**M)
      B=B*EPS*(R0**N)
      AM=A*M
      BN=B*N
      CO=CO*R0
      CO2=CO*CO
      XDIM = XF/R0
      YDIM = YF/R0
      ZDIM = ZF/R0
      WRITE(6,213) XDIM, YDIM, ZDIM
      FDZ = FDZ*DT*DT*R0
      VBZ = VBZ*DT*R0
C
C PROFILE HISTOGRAM PARAMETERS
      READ(5,108)NLAY,XHIST
108  FORMAT(I3,F6.1)
      XNLAY = NLAY
      SPAC=ZF/XNLAY
      VOLHIS = (ZF/XHIST) * YF * XF/(R0**3)
      NHIST = IFIX(XHIST+0.1)
C
C LINK CELLS
      READ(5,109) NLX, NLY, NLZ      numbers of cells in each direction
109  FORMAT(3I3)
      WRITE(6,204) NLX, NLY, NLZ
      NL2 = NLX * NLY
      NL3 = NLX * NLY * NLZ
      XNL = NLX
      YNL = NLY
      ZNL = NLZ
      CMAXX = XF/(XNL * R0)    maximum spherical pair potential cut-off allowed
      CMAXY = YF/(YNL * R0)
      CMAXZ = ZF/(ZNL * R0)
      WRITE (6,210) CMAXX,CMAXY,CMAXZ    cot off must be less than the smallest of these
C
      IF(NRUN.GE.1)GO TO 2
C LATTICE CONFIGURATION AND INITIAL VELOCITIES
      READ (5,110) NCA,NXA,NYA,NZA
110  FORMAT(4I3)
      WRITE(6,209) NCA,NXA,NYA,NZA
      XNXA = NXA/XF
      XNYA = NYA/YF
      XNZA = NZA/ZF
      I=1
      TEMPX = 0.0
      TEMPY = 0.0
      TEMPZ = 0.0
      DO 3 J=1,NCA
          READ(5,111) X0(J),Y0(J),Z0(J)
111  FORMAT(3F8.4)
          WRITE(6,211) J, X0(J),Y0(J),Z0(J)
          DO 3 IX=1,NXA

```

```

DO 3 IY=1,NYA
DO 3 IZ=1,NZA
C initial positions for a face centered cubic lattice
RX(I)=((IX-1)+X0(J))/XNXA
RY(I)=((IY-1)+Y0(J))/XNYA
RZ(I)=((IZ-1)+Z0(J))/XNZ A
C use of initial positions to generate initial random velocities (caution-equilibrate well)
VY(I) = RX(I) - 0.5*XF
VZ(I) = RY(I) - 0.5*XF
VX(I) = RZ(I) - 0.5*ZF
C initial temperatures/kinetic energies
TEMPX=TEMPX + VX(I)**2
TEMPY=TEMPY + VY(I)**2
TEMPZ=TEMPZ + VZ(I)**2
I=I+1
3 CONTINUE
TEMPX = TEMPX/(XNA * EPS)
TEMPY = TEMPY/(XNA * EPS)
TEMPZ = TEMPZ/(XNA * EPS)
C scaling factor required to renormalise temp in each direction separately
FACX = SQRT(TI/TEMPX)
FACY = SQRT(TI/TEMPY)
FACZ = SQRT(TI/TEMPZ)
GO TO 24
C
C READ IN CONFIGURATION FROM FILE 7
2 CONTINUE
FACX = 1.0
FACY = 1.0
FACZ = 1.0
DO 14 I=1,NA
READ(7,250) RX(I),RY(I),RZ(I),VX(I),VY(I),VZ(I)
C check that Y- values (slab dimension with rigid walls) are not exactly zero
IF(RY(I).LT.0.000001) RY(I) = 0.000001
IF(RY(I).GE.YF) RY(I) = YF -0.000001
14 CONTINUE
C
24 CONTINUE
C CELL OCCUPANCY TABLES
C in this code N particles are indexed according to position starting with 1-L1(1) in cell(1), L0(2)-L1(2), in
CELL(2) up to L0(N)-n in CELL (NL3)
J = 1
DO 20 IP=1,NL3 (NL3 is total number of cells NLX*NL Y*NLZ)
L0(IP) = J
L1(IP) = 0
DO 21 I= 1, NA
IX = INT( RX(I) * XNL/XF + 1.0)
IY = INT( RY(I) * YNL/YF)
IZ = INT( RZ(I) * ZNL/ZF)
ICI = IX + NLX*IY + NL2*IZ
IF(ICI.NE.IP) GO TO 21
FX(J)=RX(I)
FY(J)=RY(I)
FZ(J)=RZ(I)
L1(IP) = J
J = J + 1
21 CONTINUE
IF(L1(IP).EQ.0)L0(IP) = 0
20 CONTINUE
C
DO 96 I=1,NA
RX(I)=FX(I)

```



```

      RY(I)=FY(I)
      RZ(I)=FZ(I)
96  CONTINUE
C
C WRITE OUT CELL OCCUPANCY
      NCOUNT = 0
3999 CONTINUE
      WRITE(6,208)
      DO 69 IZ = 1,NLZ
          JZ = IZ-1
          DO 69 IY = 1,NLY
              JY = IY - 1
              DO 69 IX = 1,NLX
                  JP= IX + NLX * JY + NL2 * JZ
                  NIN(JP)=L1(JP)-L0(JP)+1
                  IF(L0(JP).EQ.0)NIN(JP) = 0
                  WRITE(6,*)JP,L0(JP),L1(JP),NIN(JP)
69  CONTINUE
C
C CHECK CELL OCCUPANCY INDEX
      DO 31 J=1,NA
          IX = INT( RX(J) * XNL/XF + 1.0)
          IY = INT( RY(J) * YNL/YF)
          IZ = INT( RZ(J) * ZNL/ZF)
          JP = IX + NLX*IY + NL2*IZ
          IF(J.GE.L0(JP).AND.J.LE.L1(JP))GO TO 31
          WRITE (6,220) J,JP,L0(JP),L1(JP)
31  CONTINUE
      IF(NCOUNT.NE.0) GO TO 998
C
C WRITE INITIAL CONFIGURATION
      TEMPX = 0.0
      TEMPY = 0.0
      TEMPZ = 0.0
      WRITE (6,214)
      DO 32 I=1,NA
          IF(I.LE.10)WRITE(6,250) RX(I),RY(I),RZ(I),VX(I),VY(I),VZ(I)
          VX(I) = VX(I) * FACX
          VY(I) = VY(I) * FACY
          VZ(I) = VZ(I) * FACZ
          TEMPX=TEMPX + VX(I)**2
          TEMPY=TEMPY + VY(I)**2
          TEMPZ=TEMPZ + VZ(I)**2
32  CONTINUE
      TEMPX = TEMPX/(XNA * EPS)
      TEMPY = TEMPY/(XNA * EPS)
      TEMPZ = TEMPZ/(XNA * EPS)
      TEMP = (TEMPX + TEMPY + TEMPZ)/3.0
      WRITE(6,207) TEMP, TEMPX, TEMPY, TEMPZ
C
C INITIAL MOMENTA
      PX=0.0
      PY=0.0
      PZ=0.0
      DO 5 I=1,NA
          PX=PX+VX(I)
          PY=PY+VY(I)
          PZ=PZ+VZ(I)
5  CONTINUE
C
C ZERO MOMENTA
      X=PX/XNA

```

```

Y=PY/XNA
Z=PZ/XNA
    TEMPX = 0.0
    TEMPY = 0.0
    TEMPZ = 0.0
DO 6 I=1,NA
VX(I)=VX(I)-X
VY(I)=VY(I)-Y
VZ(I)=VZ(I)-Z
TEMPX=TEMPX + VX(I)**2
TEMPY=TEMPY + VY(I)**2
TEMPZ=TEMPZ + VZ(I)**2
6  CONTINUE
    TEMPX = TEMPX/(XNA * EPS)
    TEMPY = TEMPY/(XNA * EPS)
    TEMPZ = TEMPZ/(XNA * EPS)
C
C ZERO ALL ACCUMULATORS
    NCOUNT = 0
    NPRINT = 0
    ZNFLOW = 0.0
    TEMPAV = 0.0
    TEMXAV = 0.0
    TEMYAV = 0.0
    TEMZAV = 0.0
    PVAV = 0.0
    UAV = 0.0
    PHIAV = 0.0
    PSIAV = 0.0
    PVSQ = 0.0
    PHISQ = 0.0
    PSISQ = 0.0
    PSIPHI = 0.0
C SET ARRAYS TO ZERO
DO 7 L= 1, 100
DEN(L) = 0.0
    VLZ(L) = 0.0
    TEE(L) = 0.0
    STR(L) = 0.0
    POT(L) = 0.0
    ZZP(L) = 0.0
7  CONTINUE
DO 25 L = 1, NLAY
    XNORM(L) = 0.0
    TEELAY(L) = 0.0
    POTLAY(L) = 0.0
    STRLAY(L) = 0.0
25  CONTINUE
DO 26 I = 1,NA
    DISPX(I) = 0.0
    DISPY(I) = 0.0
    DISPZ(I) = 0.0
26  CONTINUE
    ZNFLOW = 0.0
    ZNFLOW = 0.0
C
C SUM FORCE ON EACH ATOM
12  CONTINUE
C
C THE VELOCITIES ARE SCALED IF ISCALE=1
C EACH DIRECTION SEPERATELY
    FACX = SQRT(TI/TEMPX)

```

```

FACY = SQRT(TI/TEMPY)
FACZ = SQRT(TI/TEMPZ)
IF (ISCALE.EQ.1) GOTO 46
IF (NCOUNT.EQ.0) GOTO 46
FACX = 1.0
FACY = 1.0
FACZ = 1.0
C
46 CONTINUE
DO 8 I=1,NA
PZZ(I) = 0.0
SZ(I) = 0.0
PS(I) = 0.0
VX(I) = VX(I) * FACX
VY(I) = VY(I) * FACY
VZ(I) = VZ(I) * FACZ
8 CONTINUE
PHIM=0.0
PHIN=0.0
IP=0
DO 9 IZ = 1, NLZ
DO 9 IY = 1, NLY
DO 9 IX = 1, NLX
IP = IP + 1
C .....CELL IP EMPTY
IF (L0(IP).EQ.0) GOTO 39
C .....CALCULATE JP
JY = 1
DO 40 KX = IX-1,IX+1
DO 40 KZ = IZ-1,IZ+1
IF(KX.EQ.IX-1.AND.KZ.EQ.IZ)GO TO 40
CX = 0.0
CY = 0.0
CZ = 0.0
JX = KX
JZ = KZ
C .....PERIODIC BOUNDARY CONDITIONS
C this is a slab with rigid walls in the Y-direction and periodicity in X and Z only
IF (JX - NLX-1) 73, 70, 73
70 JX = 1
CX = XF
73 IF (JZ - NLZ-1) 75, 74, 75
74 JZ = 1
CZ = ZF
75 IF (JX) 79, 76, 79
76 JX = NLX
CX = -XF
79 IF (JZ) 82, 80, 82
80 JZ = NLZ
CZ = -ZF
C
82 JP = JX + (JY-1) * NLX + (JZ-1) * NL2
IF(L0(JP).EQ.0) GO TO 41
C
N1=L0(IP)
N2=L1(IP)
DO 19 I=N1,N2
C
XR=RX(I)
YR=RY(I)
ZR=RZ(I)
C

```

```

N3=L0(JP)
N4=L1(JP)
DO 18 J=N3,N4
IF(IP.EQ.JP.AND.I.GE.J)GO TO 18
C calculate forces between particles I (I) and j(J)
X=RX(J)-XR+CX
Y=RY(J)-YR+CY
Z=RZ(J)-ZR+CZ
XX = X*X
YY = Y*Y
ZZ = Z*Z
R2 = XX + YY + ZZ
IF(R2.GT.CO2) GOTO 18
R2 = 1.0D0/R2
RM=R2*R2*R2
RN=RM*RM
PHIN = PHIN + RN
PHIM = PHIM + RM
F = A *RM + B*RN
PS(I) = PS(I) + F
PS(J) = PS(J) + F
C
F = AM*RM + BN*RN
F=F*R2
X=F*X
Y=F*Y
Z=F*Z
FZZ = ZZ * F
SZZ = (XX-ZZ) * F
VX(I) = VX(I) - X
VY(I) = VY(I) - Y
VZ(I) = VZ(I) - Z
VX(J) = VX(J) + X
VY(J) = VY(J) + Y
VZ(J) = VZ(J) + Z
PZZ(I) = PZZ(I) - FZZ
PZZ(J) = PZZ(J) - FZZ
SZ(I) = SZ(I) + SZZ
SZ(J) = SZ(J) + SZZ
18 CONTINUE
19 CONTINUE
41 CONTINUE
40 CONTINUE
39 CONTINUE
9 CONTINUE
C
NCOUNT = NCOUNT + 1
XCOUNT = NCOUNT
C UPDATE CONFIGURATION
C
TEMP = 0.0
TEMPX= 0.0
TEMPY= 0.0
TEMPZ= 0.0
PX=0.0
PY=0.0
PZ=0.0
DO 27 L = 1,NLAY
DXSQ(L)=0.0
DYSQ(L)=0.0
DZSQ(L)=0.0
XSUM(L)=0.0

```

```

27 CONTINUE
C
DO 10 I=1,NA
C SUM MOMENTA
PX=PX+VX(I)
PY=PY+VY(I)
PZ=PZ+VZ(I)
C ACCUMULATE Z-PROFILES
K = INT(RZ(I) * XHIST/ZF) + 1
DEN(K) = DEN(K) + 1.0
VLZ(K) = VLZ(K) + VZ(I)
STR(K) = STR(K) + SZ(I)
ZZP(K) = ZZP(K) + PZZ(I)
POT(K) = POT(K) + PS(I)
C LAYER PROPERTIES
L = INT(RZ(I) * XNLAY/ZF) + 1
C DIFFUSION
DISPX(I) = DISPX(I) + VX(I)
DISPY(I) = DISPY(I) + VY(I)
DISPZ(I) = DISPZ(I) + VZ(I)
DXSQ(L) = DXSQ(L) + DISPX(I)*DISPX(I)
DYSQ(L) = DYSQ(L) + DISPY(I)*DISPY(I)
DZSQ(L) = DZSQ(L) + DISPZ(I)*DISPZ(I)
XSUM(L) = XSUM(L) + 1.0

C
EKIX = VX(I)**2
EKIY = VY(I)**2
EKIZ = VZ(I)**2
EKI = (EKIX + EKIY + EKIZ)/(3.0 * EPS)
TEE(K) = TEE(K) + EKI
TEMPX = TEMPX + EKIX/(XNA * EPS)
TEMPY = TEMPY + EKIY/(XNA * EPS)
TEMPZ = TEMPZ + EKIZ/(XNA * EPS)
TEMP = TEMP + EKI/XNA
TEELAY(L) = TEELAY(L) + EKI
POTLAY(L) = POTLAY(L) + PS(I)
STRLAY(L) = STRLAY(L) + SZ(I)
XNORM(L) = XNORM(L) + 1.0
C OLD CELL
IX = INT( RX(I) * XNL/XF + 1.0)
IY = INT( RY(I) * YNL/YF)
IZ = INT( RZ(I) * ZNL/ZF)
ICI = IX + NLX*IY + NL2*IZ
C EXTERNAL FORCE
VZ(I) = VZ(I) - FDZ
C NEW POSITIONS
RX(I) = RX(I) + VX(I)
RY(I) = RY(I) + VY(I)
RZ(I) = RZ(I) + VZ(I)
C PERIODIC BOUNDARY IN X
IF(RX(I).GE.XF) RX(I) = RX(I) - XF
IF(RX(I).LT.0.0) RX(I) = RX(I) + XF
C RIGID BOUNDARY IN Y
IF(RY(I).GE.YF) RY(I) = RY(I) - VY(I)
IF(RY(I).GE.YF) VY(I) = - VY(I)
IF(RY(I).LT.0.0) RY(I) = RY(I) - VY(I)
IF(RY(I).LT.0.0) VY(I) = - VY(I)
C RIGID BOUNDARY AT Z=ZF
IF(RZ(I).GE.ZF) VZ(I) = -VZ(I)
IF(RZ(I).GE.ZF) RZ(I) = ZF - 0.000001
IF(RZ(I).GE.0.0) GO TO 1000

```

```

C Z=0 BOUNDARY CONDITIONS
C if NVB          1=PERIODIC    2=MOVING    3=RIGID
      IF(NVB.EQ.3) GO TO 1001
      IF(NVB.EQ.1) GO TO 1002
C MOVING BOUNDARY AT Z=0
      IF(-VZ(I).GT.VBZ) GO TO 1001
1002 CONTINUE
      RZ(I) = RZ(I) + ZF
C accumulate the flow rate in the z-direction
      ZNFLOW = ZNFLOW + 1.0
      GO TO 1000
1001 CONTINUE
      RZ(I)=RZ(I)-VZ(I)
      VZ(I) = -VZ(I)
C accumulate the collision (reversal) rate at the +Z semi-permeabl boundary.
      ZNCOLL = ZNCOLL + 1.0
1000 CONTINUE
C NEW CELL
      IF(RX(I).GE.XF)RX(I) = XF - 0.000001
      IF(RY(I).GE.YF)RY(I) = YF - 0.000001
      IF(RZ(I).GE.ZF)RZ(I) = ZF - 0.000001
      IX = INT( RX(I) * XNL/XF + 1.0)
      IY = INT( RY(I) * YNL/YF)
      IZ = INT( RZ(I) * ZNL/ZF)
      IP = IX + NLX*IY + NL2*IZ
      IF(IP.LE.0.OR.IP.GT.NL3) GO TO 999
C
C UPDATE PARTICLE INDICES
C Once a particle has moved across a cell boundary, the index of all the other particles changes to restore the addressing system
for locating particles by cell. This code updates the indices of all the particles.
      IF(IP.EQ.ICI)GO TO 34
      X=RX(I)
      Y=RY(I)
      Z=RZ(I)
      XX=VX(I)
      YY=VY(I)
      ZZ=VZ(I)
      XXX = DISPX(I)
      YYY = DISPY(I)
      ZZZ = DISPZ(I)
      NIN(ICI)=NIN(ICI) -1
      NIN(IP) = NIN(IP) +1
      IF(IP.GT.ICI)GO TO 112
C
      J = L0(ICI)
      IF(L0(ICI).NE.L1(ICI))GO TO 139
      L0(ICI) = 0
      L1(ICI) = 0
139 CONTINUE
      L = ICI
      DO 117 JP = IP+1,ICI
        K = L-1
        IF(L0(L).NE.0) L0(L)= L0(L) + 1
        IF(L1(K).NE.0) L1(K)= L1(K) + 1
        IF(L0(L).NE.0) J=L0(L)-1
        L = L-1
117 CONTINUE
      IF(L1(IP).NE.0) GO TO 127
      L0(IP) = J
      L1(IP) = J
127 CONTINUE
      J=I

```

```

115 K=J-1
    IF(J.LE.L1(IP))GO TO 33
    RX(J)=RX(K)
    RY(J)=RY(K)
    RZ(J)=RZ(K)
    VX(J)=VX(K)
    VY(J)=VY(K)
    VZ(J)=VZ(K)
    DISPX(J)=DISPX(K)
    DISPY(J)=DISPY(K)
    DISPZ(J)=DISPZ(K)
    J=J-1
    GO TO 115
C
112 CONTINUE
    J = L1(ICI)
    IF(L0(ICI).NE.L1(ICI))GO TO 129
    L0(ICI) = 0
    L1(ICI) = 0
129 CONTINUE
    DO 94 L = ICI,IP-1
        K = L+1
        IF(L0(K).NE.0) L0(K)= L0(K) - 1
        IF(L1(L).NE.0) L1(L)= L1(L) - 1
        IF(L1(L).NE.0) J=L1(L)+1
94 CONTINUE
    IF(L1(IP).NE.0) GO TO 128
    L1(IP) = J
    L0(IP) = J
128 CONTINUE
    J=I
118 K=J+1
    IF(J.GE.L0(IP))GO TO 33
    RX(J)=RX(K)
    RY(J)=RY(K)
    RZ(J)=RZ(K)
    VX(J)=VX(K)
    VY(J)=VY(K)
    VZ(J)=VZ(K)
    DISPX(J)=DISPX(K)
    DISPY(J)=DISPY(K)
    DISPZ(J)=DISPZ(K)
    J=J+1
    GO TO 118
C
33 CONTINUE
    RX(J)=X
    RY(J)=Y
    RZ(J)=Z
    VX(J)=XX
    VY(J)=YY
    VZ(J)=ZZ
    DISPX(J)=XXX
    DISPY(J)=YYY
    DISPZ(J)=ZZZ
34 CONTINUE
10 CONTINUE
C
C ACCUMULATE TIME AVERAGES
C
    PHIM=A*PHIM/(EPS*XNA)
    PHIN=B*PHIN/(EPS*XNA)

```

```

PSI=-(M*PHIM + N*PHIN)
PHI=PHIN+PHIM
U = PHI+1.5*TEMP
PV = 1.0-PSI/(TEMP*3.0)
TEMPAV = TEMPAV + TEMP
TEMXAV = TEMXAV + TEMPX
TEMYAV = TEMYAV + TEMPY
TEMZAV = TEMZAV + TEMPZ
UAV = UAV + U
PVAV = PVAV + PV
PHIAV = PHIAV + PHI
PSIAV = PSIAV + PSI
PHISQ = PHISQ + PHI * PHI
PSISQ = PSISQ + PSI * PSI
PSIPHI = PSIPHI + PSI * PHI
C
C REGULAR PRINT OUT EVERY NPRINT TIME STEPS
C
  IF(NCOUNT.EQ.1) GO TO 61
    IF(NSUB.EQ.1) GO TO 61
    IF(NCOUNT.EQ.NPRINT) GO TO 61
    GO TO 60
61  CONTINUE
    WRITE(6,205) NCOUNT, PX, PY, PZ, U, PHIM, PHIN, PV
    WRITE(6,207) TEMP, TEMPX, TEMPY, TEMPZ
C
  IF(NRUN.EQ.0)GO TO 56
  DO 55 L= NLAY,1,-1
    XMSD = DXSQ(L)/(XSUM(L)*R0*R0)
    YMSD = DYSQ(L)/(XSUM(L)*R0*R0)
    ZMSD = DZSQ(L)/(XSUM(L)*R0*R0)
    DX = XMSD/(2.0*XNSUB*DT)
    DY = YMSD/(2.0*XNSUB*DT)
    DZ = ZMSD/(2.0*XNSUB*DT)
    WRITE(6,450)L,DX,DY,DZ
55  CONTINUE
    DO 30 I = 1,NA
      DISPX(I) = 0.0
      DISPY(I) = 0.0
      DISPZ(I) = 0.0
30  CONTINUE
C
C RATE OF FLUX
56  CONTINUE
    X = ZNFLOW*R0*R0/(XNSUB*DT)
    WRITE(6,216)ZNFLOW,X,ZNCOLL
    ZNFLOW = 0.0
    ZNCOLL = 0.0
C
    NPRINT = NPRINT + NSUB
C
60  CONTINUE
    IF(NCOUNT.GE.NDT) GOTO 11
    GOTO 12
C
C END OF RUN
11  CONTINUE
C FINAL AVERAGES
    TEMPAV = TEMPAV / XCOUNT
    TEMXAV = TEMXAV / XCOUNT
    TEMYAV = TEMYAV / XCOUNT
    TEMZAV = TEMZAV / XCOUNT

```

average temperature

PVAV = PVAV / XCOUNT	average pressure ($\langle p_v / NkT \rangle$)
UAV = UAV / XCOUNT	average internal energy
PHIAV = PHIAV / XCOUNT	average potential energy
PSIAV = PSIAV / XCOUNT	average virial
PVSQ = PVSQ / XCOUNT	mean square pressure
PHISQ = PHISQ / XCOUNT	mean square potential
PSISQ = PSISQ / XCOUNT	mean square virial
PSIPHI = PSIPHI / XCOUNT	covariance potential-virial

```

WRITE (6,355) NCOUNT
WRITE (6,360) UAV
WRITE (6,370) TEMPAV
WRITE (6,380) PVAV
WRITE (6,390) PHIAV
WRITE (6,400) PSIAV
WRITE (6,420) PHISQ
WRITE (6,430) PSISQ
WRITE (6,440) PSIPHI
WRITE (6,460) TEMXAV
WRITE (6,470) TEMYAV
WRITE (6,480) TEMZAV
WRITE (6,280)
C
C NORMALISE AND PRINT OUT Z-PROFILES
C
DO 35 L = NHIST,1,-1
  Z = (ZF/XHIST) * (L - 1)/R0
  D = DEN(L)/(XCOUNT * VOLHIS)
  V = VLZ(L)/(DEN(L)*DT*R0)
  W = D*V
  IF (D.GT.0.00000001) GOTO 42
  S = 0.0
  T = 0.0
  P = 0.0
  F = 0.0
  GOTO 43
42  S = -STR(L)/(XCOUNT * 2.0 * EPS * VOLHIS)
    T = TEE(L)/DEN(L)
    P = POT(L)/(DEN(L) * 2.0 * EPS)
    F = D * T - ZZP(L)/(VOLHIS * 2.0 * XCOUNT * EPS)
43  WRITE(6,290)L,Z,D,V,W,T,P,S,F
35  CONTINUE
C
C RMSD POTENTIAL AND KINETIC ENERGIES PER LAYER
C
WRITE(6,320)
DO 36 L= NLAY,1,-1
  IF(XSUM(L).EQ.0) GO TO 36
  XMSD = DXSQ(L)/(XSUM(L)*R0*R0)
  YMSD = DYSQ(L)/(XSUM(L)*R0*R0)
  ZMSD = DZSQ(L)/(XSUM(L)*R0*R0)
  DX = XMSD**0.5
  DY = YMSD**0.5
  DZ = ZMSD**0.5
  TLAY = TEELAY(L)/(XNORM(L))
  PLAY = POTLAY(L)/(XNORM(L) * 2.0 * EPS)
  SLAY = STRLAY(L)/(XNORM(L) * 2.0 * EPS * VOLHIS)
  WRITE(6,300) L, DX, DY, DZ, TLAY, PLAY, SLAY
36  CONTINUE
C WRITE OUT FINAL CONFIGURATION
REWIND 7
DO 13 I=1,NA
  IF(RY(I).LT.0.000001) RY(I) = 0.000001

```

```

        IF(RY(I).GE.YF) RY(I) = YF -0.000001
        WRITE(7,250) RX(I),RY(I),RZ(I),VX(I),VY(I),VZ(I)
13  CONTINUE
        WRITE(6,215)
        DO 37 I=1,50
            WRITE(6,250) RX(I),RY(I),RZ(I),VX(I),VY(I),VZ(I)
37  CONTINUE
C
C FORMAT WRITE STATEMENTS
C
200  FORMAT(/,'n-m PARAMETERS',2(I3),6X,'A B',2(F6.2),2X,'CO=',F5.2,/)
201  FORMAT("RHO=",F8.4,4X,"TI=",F8.4,4X,'FDZ=',F8.4,4X,'VBZ=',F8.4,/)
202  FORMAT('NUMBER of PARTICLES =',I6,/)
203  FORMAT('NRUN=',I3,4X,'NDT=',2I8,4X,'DT=',F8.4,4X,'ISCALE=',I3,/)
204  FORMAT('NLX=',I2,2X,'NLY=',I2,2X,'NLZ=',I2,/)
205  FORMAT(/,'TIME',I8,' PX PY PZ',3(E9.3),2X,'U',3F7.3,2X,'Z',F8.3)
206  FORMAT('BOX DIMENSIONS XF YF ZF',3F8.4,/)
207  FORMAT('TEMP',F8.4,2X,'TX TY TZ',3(2X,F8.4))
208  FORMAT(/,'CHECK ON LINK CELL ARRAYS',/)
209  FORMAT(/,I3,' ATOMS IN UNIT CELL',3I3,/)
210  FORMAT('CMAX X Y Z are',3(F8.4)/)
211  FORMAT('C0-ORDS XYZ',I2,3F8.4)
213  FORMAT('XDIM=',F8.4,2X,'YDIM=',F8.4,2X,'ZDIM=',F8.4,/)
214  FORMAT(/,'INITIAL CONFIGURATION',/)
215  FORMAT(/,'FINAL CONFIGURATION',/)
216  FORMAT('ZNFLOW=',F10.0,2X,E11.4,8X,'ZNCOLL=',F10.0,/)
220  FORMAT("OUT OF CELL",I6,3(2X,I5),/)
221  FORMAT(/,'PERIODIC BOUNDARY AT Z=0',/)
222  FORMAT(/,'MOVING BOUNDARY AT Z=0',/)
223  FORMAT(/,'RIGID BOUNDARY AT Z=0',/)
250  FORMAT(3F10.6,2X,3E12.4)
280  FORMAT(/,8X,'Z/ro',4X,'RHO',6X,'VZ',6X,'flux',6X,' KE',
        16X,'PE',6X,'STRESS',4X,'PZZ',/)
290  FORMAT(I4,F8.2,11(F9.3))
300  FORMAT(I5,6(4X,F8.4))
320  FORMAT(/,'LAYER',6X,'RMSDX',7X,'RMSDY',7X,'RMSDZ',7X,'TEELAY',6X,
        1'POTLAY',6X,'STRLAY',/)
355  FORMAT(/,'TIME AVERAGES',6X,'NCOUNT=',I8,/)
360  FORMAT(' ENERGY = ',F10.4)
370  FORMAT(' TEMP = ',F10.4)
380  FORMAT(' PRESSURE = ',F10.4)
390  FORMAT(' POTENTIAL = ',F10.4)
400  FORMAT(' VIRIAL = ',F10.4)
420  FORMAT(' MSQ POT = ',F10.4)
430  FORMAT(' MSQ VIRIAL = ',F10.4)
440  FORMAT(' Av PSIPHI = ',F10.4)
460  FORMAT(' TEMP X = ',F10.4)
470  FORMAT(' TEMP Y = ',F10.4)
480  FORMAT(' TEMP Z = ',F10.4)
450  FORMAT(10X,I2,' DX DY DZ',3F8.4)
        GO TO 998
C POSTMORTEM
999  CONTINUE
        WRITE(6,2999)NCOUNT,I,J,IX,IY,IZ,IP,ICI
2999  FORMAT(/,'POSTMORTEM',8I6,/)
        WRITE(6,*)RX(I),RY(I),RZ(I),VX(I),VY(I),VZ(I)
        GO TO 3999
998  CONTINUE
        STOP
        END

```

APPENDIX II

Reagents procured for first single batch (0.5l@50%) monodisperse polystyrene latex:
 Almog dispersion polymerization method (8), prescription according to Liu et al (9,10)

CHEMICAL DESCRIPTION	QUANTITY	COST
Poly(Ethylene glycol)methyl ether (2000)	250 g	35.00
11-bromoundecanol	50 g	50.00
p-toluenesulfonic acid monohydrate	100 g	6.00
THF anhydrous	1 L	37.00
Ether	2.5 L	19.00
Chloroform-distilled	2.0 L	17.00
Methacryloyl chloride	100 ml	24.00
Azobisisobutyronitrile (AIBN)	100 g	12.00
Styrene	2.5 L	24.00
Methanol	2.5 L	12.00
Dichloromethane	2.5 L	15.00
3,4-dihydro-2H-pyran	100 ml	10.00
Magnesium Sulphate	500 g	7.00
Ethanol	2.0 L	20.00
Potassium Hydroxide	500 g	7.00
Molecular Sieves, 3A, 5A, 4A	3x500 g	45.00
Triethylamine	100 ml	9.00
Toluene anhydrous	2.0 L	35.00
Chloroform (CDCl ₃)	2.0 L	17.00